Fusion Engineering and Design 87 (2012) 853–858

Contents lists available at SciVerse ScienceDirect

Fusion Engineering and Design

journal homepage: www.elsevier.com/locate/fusengdes

Mechanics of binary and polydisperse spherical pebble assembly

R.K. Annabattula[a,*], Y. Gan[b], M. Kamlah[a]

[a] Institute for Applied Materials (IAM-WBM), Karlsruhe Institute of Technology (KIT), D-76344, Eggenstein-Leopoldshafen, Germany
[b] School of Civil Engineering, The University of Sydney, 2006 NSW, Sydney, Australia

ARTICLE INFO

Article history:
Available online 22 March 2012

Keywords:
Nuclear fusion
Polydisperse granular mechanics
Discrete element method
Pebble bed thermomechanics

ABSTRACT

The micromechanical behavior of an assembly of binary and polydisperse spherical pebbles is studied using discrete element method (DEM) accounting for microscopic interactions between individual pebbles. A in-house DEM code has been used to simulate the assemblies consisting of different pebble diameters and the results of the simulations are compared with that of mono-size pebble assemblies. The effect of relative radii and volume fraction of the pebbles on the macroscopic stress–strain response is discussed. Furthermore, the effect of packing factor and coefficient of friction on the overall stress–strain behavior of the system is studied in detail. The shear (tangential) stiffness between the particles is also another influencing parameter. For a very small shear stiffness the system shows a strong dependence on the packing factor while a pebble material dependent shear stiffness shows a rather moderate dependence on the packing factor. For a similar packing factor, the mono-size assembly shows a stiff behavior during loading compared to binary assembly. However, the simulations do not show a significant difference between the two behaviors in contrast to the observations made in the experiments. The discrepancy can be attributed to (i) probable difference in packing factors for mono-size and binary assemblies in the experiments, (ii) arbitrary friction coefficient in the current model and (iii) the tangential interaction (constant shear stiffness) implemented in the present model which needs further modification as a function of the load history on the pebbles. Evolution of other micromechanical characteristics such as coordination number, contact force distribution and stored elastic energy of individual pebbles as a function of external load and system parameters is presented which can be used to estimate important macroscopic properties such as overall thermal conductivity and crushing resistance of the pebble beds.

1. Introduction

Tritium breeding and neutron multiplication are two primary goals for a sustained fusion fuel cycle in fusion reactors. These two goals are achieved by breeding blankets either in liquid or solid form. Solid breeding blankets comprise of ceramic breeder material such as lithium-ortho-silicate (OSi) or lithium-meta-titanate (MTi) and beryllium (Be) as neutron multipliers both in the form of pebble beds. Knowledge of the structural integrity as well as the thermo-mechanical behavior of these pebble beds is extremely important to guarantee a sustained fuel cycle [1]. The thermo-mechanical behavior of the pebble beds can be studied under two different length scales based on continuum and discrete particle methods. The former method employs a phenomenological constitutive behavior [2] to obtain a macroscopic response of the system while the later approach is aimed at investigating the micro-mechanical interactions between the individual pebbles so as to establish a link with the macroscopic thermo-mechanical response of the pebble beds. The discrete element method (DEM) has been used to study the micro-mechanical behavior of granular assemblies [3] in many fields of engineering. The application of DEM to thermo-mechanical behavior of pebble assemblies has been carried out in the past [4,5]. However, in these studies a uniform pebble size has been considered. But, the produced pebbles are known to have a diameter distribution in the range of 0.25–0.65 mm [6]. Hence, it is important to study the influence of size distribution on the overall thermo-mechanical response of the pebble assembly. To accomplish this task, we first study a binary assembly with different radius and relative volume fractions. Later, a polydisperse pebble assembly is generated conforming to the experimental pebble size distribution. The effect of packing factor, pebble size distribution and the friction between the pebbles on the macroscopic and the microscopic behavior will be investigated.

The outline of the article is as follows. In Section 2, the model and the simulation procedure will be presented. In Section 3.1, pebble assemblies with binary distribution will be studied and in Section 3.2 the results concerning the polydisperse pebble assemblies will be presented. Finally, we conclude the article in Section 4.

* Corresponding author.
E-mail addresses: ratna.annabattula@kit.edu (R.K. Annabattula), yixiang.gan@sydney.edu.au (Y. Gan), marc.kamlah@kit.edu (M. Kamlah).

0920-3796/$ – see front matter © 2012 Elsevier B.V. All rights reserved.
doi:10.1016/j.fusengdes.2012.02.033

2. Model and simulation procedure

We consider an assembly of 5000 pebbles in a periodic box of size $L \times L \times L$ as the representative volume element (RVE) for the pebble beds of much larger size. Then we apply macroscopic uni-axial strain of 1.5% on the periodic box and then unload the system to a stress-free state. The pebbles are assumed to be spherical in shape in agreement with the experiments conducted on Li_4SiO_4 pebbles [7]. The elastic modulus (E) of the OSi pebble is taken as 90 GPa and the Poisson's ratio (ν) is equal to 0.25. The pebble–pebble interaction is assumed to be elastic with normal and tangential interactions. The normal contact force is calculated based on the Hertzian contact law and the tangential contact force is taken as the minimum of the friction force and shear force calculated from the shear stiffness which is dependent on the elastic properties of the contacting pebbles [7]. The coefficient of friction (μ) between the pebbles is assumed to be equal to 0.1.

The macroscopic response of a granular assembly is characterized by the average stress of the assembly defined as [8]

$$\sigma_{ij} = \frac{1}{V}\left(\sum_{I<J}\delta^{(I,J)}f_N^{(I,J)}n_i n_j + \sum_{I<J}\delta^{(I,J)}f_T^{(I,J)}n_i t_j\right), \tag{1}$$

where $\delta^{(I,J)}$ is the distance between the centers of pebble I and J, $f_N^{(I,J)}$ and $f_T^{(I,J)}$ are the normal and shear contact forces, respectively, on pebble I exerted by pebble J, n_i and t_i denote unit vectors for directions of the normal and tangential forces, respectively. The packing factor (η) and an average pebble radius $\langle r\rangle$ for a polydisperse assembly can be written as

$$\eta = \frac{4\pi}{3V}\sum_{p=1}^{P}N_p r_p^3; \quad \langle r\rangle = \sqrt[3]{\sum_{p=1}^{P}\frac{N_p}{N}r_p^3}, \tag{2}$$

where N_p is the number of pebbles with a radius r_p in a polydisperse assembly with P different pebble sizes. We have

$$\eta = \frac{4\pi\langle r\rangle^3 N}{3V}. \tag{3}$$

The average normal contact force in the assembly can be written as

$$f_{ave} = 2\frac{\sum_{I<J}f_N^{(I,J)}}{n_c N}, \tag{4}$$

where, n_c denotes the coordination number. The hydrostatic pressure in the assembly is defined as $\sigma_{ii}/3$ given by

$$p = \frac{\sigma_{ii}}{3} = \frac{1}{3V}\left(\sum_{I<J}\delta^{(I,J)}f_N^{(I,J)}\right), \tag{5}$$

obtained by substituting $n_i n_i = 1$ and $n_i t_i = 0$ in Eq. (1). Now, combining Eqs. (3) and (4) and substituting in Eq. (5), we get

$$p = \frac{n_c\eta}{8\pi\langle r\rangle^3}f_{ave}\,\delta^*; \quad \delta^* = \frac{\sum_{I<J}\delta^{(I,J)}f_N^{(I,J)}}{\sum_{I<J}f_N^{(I,J)}}. \tag{6}$$

The term δ^* in the above expression is the length scale of the size distribution which distinguishes a mono size assembly from a polydisperse (or binary) assembly. For a mono-size assembly, $\langle r\rangle^3 = r^3$ and $\delta^{(I,J)} \simeq 2r$, so that the hydrostatic pressure $p = n_c\eta f_{ave}/(4\pi r^2)$.

3. Results

In this section, we present the results of the DEM simulations carried out for binary and polydisperse pebble assemblies. We study the effect of various parameters such as packing factor (η), coefficient of friction (μ) between the pebbles and pebble size distribution on the macroscopic average stress–strain response of the pebble assembly as well as on the interaction between the microscopic and macroscopic properties.

3.1. Binary pebble assembly

The binary pebble assemblies studied in this paper are characterized by two parameters: radius ratio (r^*) and relative volume fraction (V^*) defined as

$$r^* = \frac{r_s}{r_g}; \quad V^* = \frac{V_g}{V_s + V_g}, \tag{7}$$

where r_g and r_s are the radius of large and small pebble, respectively. V_g and V_s are the volumes occupied by the total number of large (N_g) and small pebbles (N_s), respectively given by

$$V_g = N_g\frac{4}{3}\pi r_g^3; \quad V_s = N_s\frac{4}{3}\pi r_s^3. \tag{8}$$

Fig. 1(a) shows the average stress–strain response in the loading direction (see z in Fig. 2 or indicated by stress/strain component "33") of a binary assembly characterized by $r^* = 0.6$ and $V^* = 0.7$ with different packing factors. The pebble assembly is uni-axially compressed up to 1.5% strain and then unloaded to a stress-free configuration. The assembly exhibits a stiffer response with increase in packing factor. For the case of $\eta = 0.660$ (solid line) and 0.651 (dashed line), unloading the assembly does not show a significant residual strain while for the assembly with a loose packing ($\eta = 0.643$, dotted line), the unloading curve shows a residual strain ($\approx$0.35%). This suggests that the reversibility of the system depends on the initial packing factor of the assembly. For an assembly with large packing factor, the individual pebbles have less freedom to move/rearrange during loading. For the loosely packed assemblies, the pebbles undergo considerable rearrangement during loading and hence the unloading of the system results in a new stress-free configuration different from the initial configuration leaving a net residual strain. This irreversible strain may result in a gap formation inside the blanket during thermo-mechanical cycles under operational conditions.

Fig. 1(b) shows the stress–strain response for a binary assembly with $r^* = 0.6$ for three different relative volume fractions V^*: 0.2 (solid line), 0.4 (dashed line) and 0.7 (dotted line). Clearly, for the assembly with large relative volume fraction (dotted line corresponding to $V^* = 0.7$), the response is soft compared to the assembly with lower V^* values (solid (0.2) and dashed (0.4) curves). A considerable difference in macroscopic response has not been observed for the dashed and dotted curves despite the difference in relative volume fractions. Note that the packing factor associated with each assembly analyzed above is different.[1] It is known that the stress–strain response is very sensitive to packing factor [5] and hence its effect is also expected to be present in the results. For instance, assume that the effect of relative volume fraction V^* is negligible. Then, the assembly with a high packing factor should show a stiffer response (conform Fig. 1(a)). Hence in the above Fig. 1(b), the assembly with $\eta = 0.651$ (dotted line) should show stiffer response compared with other two assemblies. But the system shows an opposite behavior. Similarly, despite the difference in packing factors the dashed and dotted lines shows almost the same behavior nullifying the effect of packing factor. This suggests that the counter intuitive behavior of the assemblies studied above should be arising from the difference in the values of relative volume fraction V^*. The

[1] It should be noted that the assemblies in this study are generated using a random close packing algorithm [9] and hence it is not possible to generate two binary assemblies of different r^* and V^* values with exactly the same packing factor.

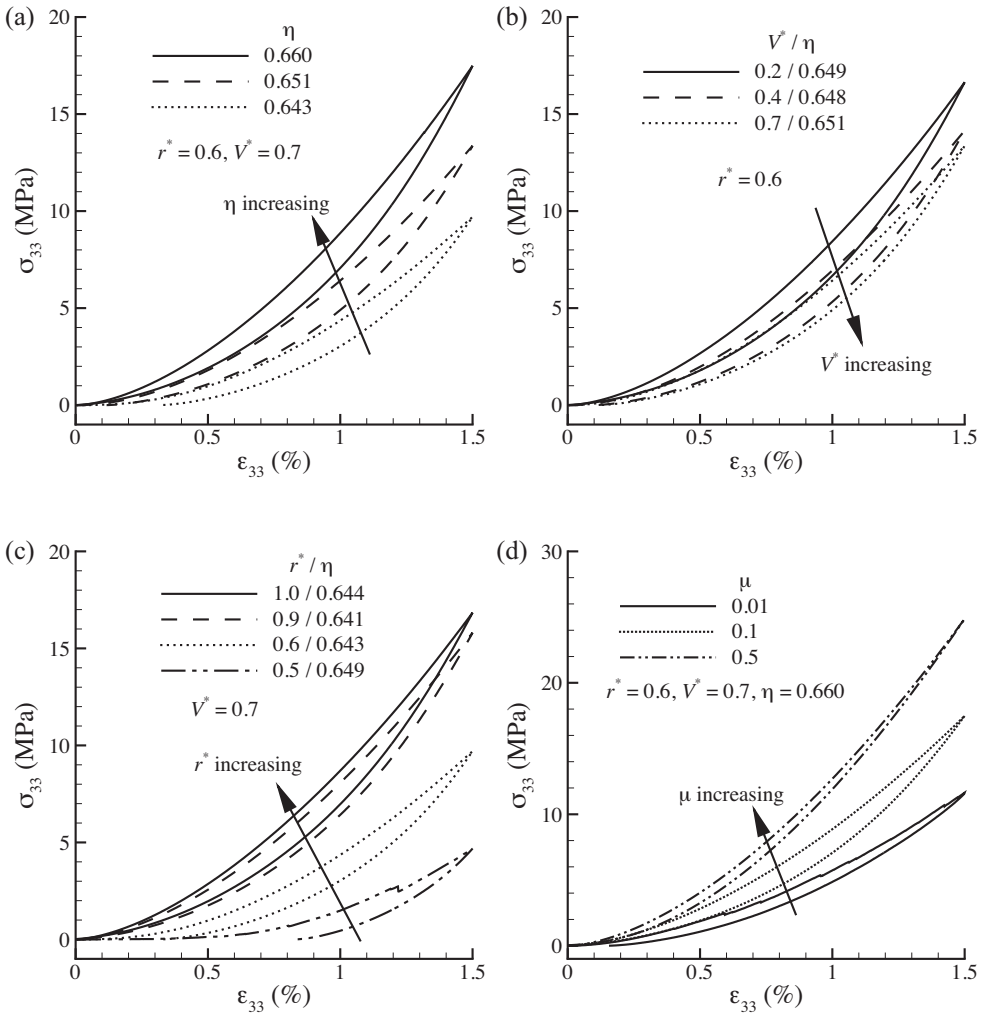

Fig. 1. Average stress–strain response of binary pebble assemblies for different packing factors (a), relative volume fractions (b), radius ratios (c) and coefficients of friction (d).

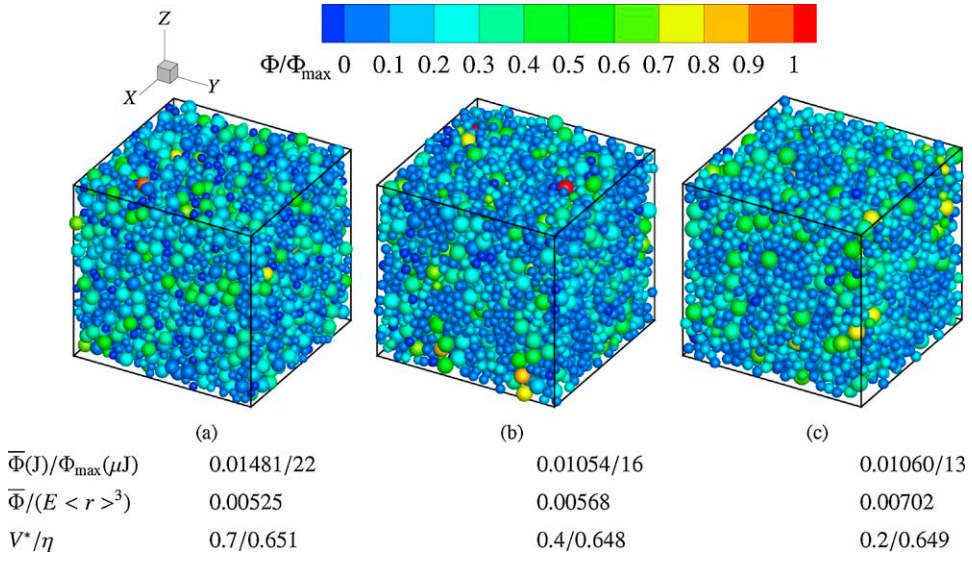

	(a)	(b)	(c)
$\overline{\Phi}(J)/\Phi_{max}(\mu J)$	0.01481/22	0.01054/16	0.01060/13
$\overline{\Phi}/(E < r >^3)$	0.00525	0.00568	0.00702
V^*/η	0.7/0.651	0.4/0.648	0.2/0.649

Fig. 2. Configurations of binary pebble assemblies with $r^* = 0.6$ for different relative volume fractions V^*: 0.7 (first column), 0.4 (second column) and 0.2 (third column) at the end of loading to 1.5% strain. Color of the each pebble corresponds to the potential energy of the pebble Φ normalized with the maximum potential energy Φ_{max} attained by a pebble in the assembly at 1.5% strain.

presence of small pebbles between two large pebbles introduces a ball-bearing like effect also observed in experiments [10] resulting in a softer response. A large value of V^* indicates the presence of more such ball-bearing like sites in the assembly resulting in a complaint behavior of the assembly.

Fig. 1(c) shows the stress–strain response for binary assemblies with different radius ratios (r^*) but with same relative volume fraction (V^*), friction coefficient (μ) and approximately same packing factor. Clearly, the stress–strain response approaches that of the mono-size (solid line) assembly as the radii of the two pebbles approach the same value (i.e., $r^* \rightarrow 1$). With the reduction in r^* value, the response becomes more complaint. This can be again referred back to the ball-bearing like behavior of small pebbles between large pebbles. A smaller value of r^* grants more freedom for small pebbles to move between the large particles thus resulting in a complaint behavior. Furthermore, the residual strain after unloading increases with decrease in r^* due to large irreversibility introduced during loading through the free movement of small pebbles.

Fig. 1(d) shows the effect of friction coefficient (μ) on the stress–strain response of the pebble assembly with $r^* = 0.6$, $V^* = 0.7$ and $\eta = 0.660$. With increase in friction coefficient, the pebbles will have less freedom to move and hence the rearrangement during loading becomes difficult leading to a stiff behavior and consequently the assembly exhibits a very small residual strain after unloading. A small value of coefficient of friction (μ) allows the pebbles to move and rearrange rigorously within the assembly thus exhibiting a complaint behavior together with a large residual strain after unloading to a stress-free state as shown in the figure.

Fig. 2 shows the potential energy (at the end of loading to 1.5% strain) in the pebbles for three binary assemblies with different relative volume fractions: 0.7 (Fig. 2(a)), 0.4 (Fig. 2(b)) and 0.2 (Fig. 2(c)). The colors of the pebbles represent the potential energy (Φ) of the pebble normalized with the maximum potential energy (Φ_{max}) attained by a pebble in the assembly. The packing factors of the three assemblies are slightly different from each other. However, it was mentioned before (see Fig. 1(b) and the corresponding discussion) that the effect of packing factor is much less pronounced (in the range of values considered here) compared to the effect of relative volume fraction V^* varying between 0.2 and 0.7. It can be clearly seen that the total potential energy of the assembly is mainly contributed by the larger pebbles while the contribution of small pebbles is relatively small. At the bottom of each column, the total potential energy of the assembly $\overline{\Phi}$ (in J) and the maximum value of the potential energy (Φ_{max}) amongst all the pebbles at $\epsilon_{33} = 1.5\%$ are mentioned. Clearly, the values of $\overline{\Phi}$ and Φ_{max} decrease with decrease in V^* showing an opposing trend to the stress-state of the assembly as a function of V^*. But, when the total energy is normalized with $E\langle r\rangle^3$, the normalized total potential energy of the assembly shows a correlation with the stress–strain response. This suggests that the interpretation of energy results should be made based on the normalized total potential energy rather than the total potential energy of the assembly.

Fig. 3(a) shows the normalized average normal force plotted against the hydrostatic pressure in a pebble assembly for different V^* values. The average normal force f_{ave} is normalized with $E < r >^2$, where <r> is an average pebble radius for the binary assembly (see Eq. (2)). Similar to the mono-size pebble assembly [5], the binary assembly also shows a unique linear dependence of the normalized average normal force with the hydrostatic pressure, independent of the relative volume fraction. Indeed, the linear relation also holds good for different values of r^* and packing factors resulting in a master curve shown in Fig. 3(a). In addition to the striking linear dependence of the normalized normal contact force on the hydrostatic pressure, the master curve also provides more insight into the average stress–strain behavior of the assemblies studied in Fig. 1. For instance, the stress state in the assembly is directly connected to the state of hydrostatic pressure of the assembly. Fig. 3(a) shows that the assembly with large value of V^* has small hydrostatic pressure which explains the soft response of the assembly with large V^* (circles) despite a large packing factor than the assembly with small V^* (squares). The average coordination number n_c of a pebble assembly is defined as the ratio of the total number of contacts to the total number of pebbles in the assembly. Fig. 3(b) shows the effect of V^* on the coordination number. The coordination number at a given hydrostatic pressure decreases with increase in V^* value in confirmation with the soft behavior of the assembly with increase in V^* value (conform Fig. 1(b)). For an assembly with a given r^* and V^* values, the coordination number increases with increase in packing factor for a given hydrostatic pressure (results not shown). Also, for a given V^*, η values and at a given hydrostatic pressure, the coordination number n_c increases with increase in r^* value (results not shown). Clearly, the coordination number is a function of r^* and V^* values in addition to hydrostatic pressure in contrast to the mono-size assemblies [5].

3.2. Polydisperse pebble assembly

In this section, we analyze the polydisperse pebble assemblies with a size (diameter) distribution between 0.25 mm and 0.65 mm as shown in Fig. 4(a). Packing of the pebble beds with such a size distribution is not a common practice in the present pebble bed designs. However, analyzing systems with a generic pebble size distribution is interesting to understand the micromechanical features for future pebble bed designs. We analyzed the average stress–strain response of the 4 batches of the polydisperse assemblies with the similar size distribution with a small variation measured in the *fusion materials laboratory* at the Karlsruhe Institute of Technology (KIT). The assemblies for DEM simulations have been generated using a modified RCP algorithm [9]. The effect of packing factor on the average stress–strain response is similar to the case of mono size and binary assemblies. The residual strain after unloading increases with decrease in packing factor akin to the observation made in binary assemblies due to ensuing irreversibility in the system.

Fig. 4(b) shows the average stress–strain response of a mono-size, binary and polydisperse assemblies. Despite having the lowest packing factor amongst the group, the mono size assembly shows a stiff behavior with negligible residual strain after unloading. On the contrary, the binary and polydisperse assemblies exhibit a rather soft behavior (in comparison to mono size assembly) along with a residual strain of approximately 0.3%. In the uni-axial compression tests carried out by [10], the assembly shows a rather soft behavior with a residual strain of approximately 0.35%. However, in the present study of polydisperse pebble assemblies, a much stiffer response during loading is observed. In the present analysis, we have assumed an arbitrary friction coefficient ($\mu = 0.1$) and it has been shown in Fig. 1(d) that it can have profound influence on the stress–strain response of the assembly. Hence, a one-to-one correspondence between the experiments and simulations can be made better with a reasonable estimate of the friction coefficient.

The master curve of scaled average normal force of binary assembly (Fig. 3(a)) may be also extended to the polydisperse assemblies since they are only distinguished by the window of size distribution. Fig. 5(a) shows the scaled average normal force as a function of hydrostatic pressure for binary and polydisperse assemblies for different combinations of size distribution amalyzed in this paper. Clearly, a unique linear dependence is observed with a very small scatter. It should be noted that the unscaled average normal force plotted against hydrostatic pressure for all the assemblies does not result in a master line as shown above. The small

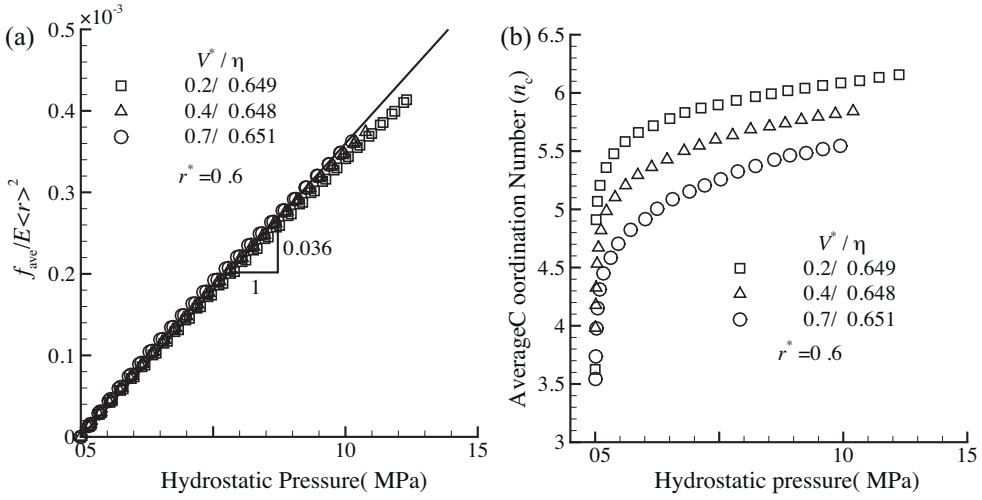

Fig. 3. Normalized average normal contact force (a) and average coordination number n_c (b) plotted against hydrostatic pressure for assemblies with $r^* = 0.6$ and approximately same packing factor for different V^* values. The average normal force of the assembly f_{ave} is normalized with $E\langle r\rangle^2$, where $\langle r\rangle$ is the average pebble radius of the pebble assembly.

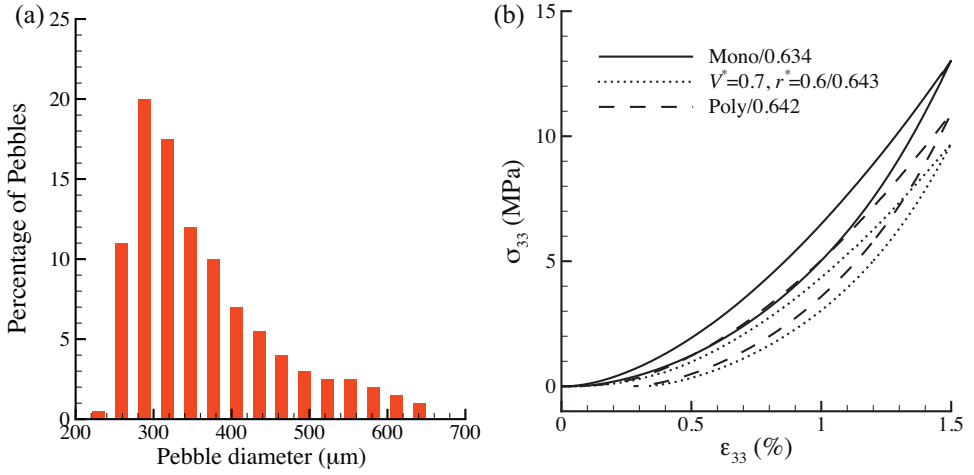

Fig. 4. (a) Pebble size distribution in a polydisperse pebble assembly. (b) Comparison of the average stress–strain response of the mono size (solid line), binary (dotted line) and polydisperse (dashed line) pebble assemblies with approximately same packing factor. The exact values of the packing factors are shown in the legend.

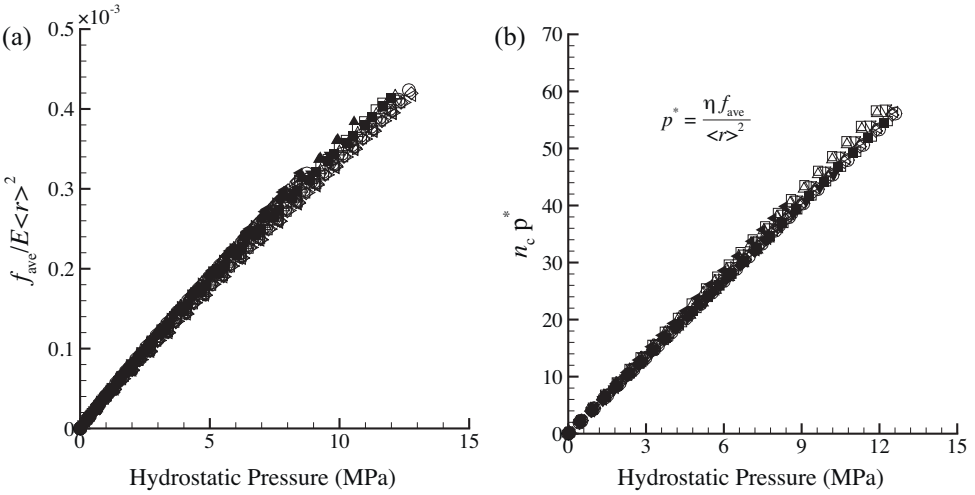

Fig. 5. (a) Normalized average normal contact force as a function of hydrostatic pressure. (b) Scaled coordination number (n_c) plotted as a function of hydrostatic pressure. The data points correspond to all the simulations carried out on binary and polydisperse assemblies with different size distributions and packing factors.

scatter about master curve for some data points may be related to the length scale of size distribution (δ^*). Similarly, the scaled average coordination number $n_c p^*$ shows a unique linear dependence with the hydrostatic pressure resulting in another master curve in Fig. 5(b). These master curves can be used to describe the micro-mechanical properties of a polydisperse assembly irrespective of the pebble size distribution and packing factor. Furthermore, these master curves show a unique relation between the microscopic properties (such as average normal force and average coordination number) and macroscopic properties (such as hydrostatic pressure) allowing them to be used as design tools for pebble beds.

4. Summary and conclusions

In summary, we have presented a numerical model based on DEM to study the micromechanics of binary and polydisperse pebble assemblies. The analysis of binary pebble assemblies shows that the average stress–strain behavior is dependent on two parameters: radius ratio r^* and relative volume fraction V^* in addition to the packing factor η. The small pebbles act like ball bearings between large pebbles resulting in an overall complaint response of the assembly. Increasing the difference between the pebble radii (i.e., decreasing r^*) or increasing the relative volume fraction of large pebbles (i.e., increasing V^*) results in complaint response of the assembly. For the same physical properties of the pebble material, the mono-size assembly shows a stiffer response compared to polydisperse and binary assemblies. Furthermore, the residual strain after unloading in polydisperse assemblies matches closely with the experimental results while the mono-size assemblies do not show any significant residual strain after unloading. The effect of friction between pebbles also plays an important role in the overall stress–strain behavior. Despite the difference in pebble size distribution the scaled average normal contact force and scaled average coordination number shows a unique linear dependence on the hydrostatic pressure resulting in two master curves. These master curves can be used to predict the micro-mechanical response of the assemblies irrespective of the pebble size distribution and packing factor in addition to establishing a link between microscopic properties and macroscopic system response.

Acknowledgments

This work supported by the European communities under the contract of Association between EURATOM and Karlsruhe Institute of Technology was carried out within the framework of the European Fusion Development Agreement. The views and opinions expressed herein do not necessarily reflect those of the European Commission. The authors would like to thank R. Knitter for providing the data on pebble size distribution and J. Reimann for fruitful discussions.

References

[1] J. Reimann, L. Boccaccini, M. Enoeda, A. Ying, Thermomechanics of solid breeder and Be pebble bed materials, Fusion Engineering and Design 61–62 (2002) 319–331.
[2] Y. Gan, M. Kamlah, Identification of material parameters of a thermomechanical model for pebble beds in fusion bblankets, Fusion Engineering and Design 82 (2007) 189–206.
[3] P.A. Cundall, O.D.L. Strack, A discrete numerical model for granular assemblies, Geotechnique 29 (1) (1979) 47–65.
[4] Z. An, A. Ying, M. Abdou, Application of discrete element method to study mechanical behaviors of ceramic breeder pebble beds, Fusion Engineering and Design 82 (2007) 2233–2238.
[5] Y. Gan, M. Kamlah, Discrete element modelling of pebble beds: with application to uniaxial compression tests of ceramic breeder pebble beds, Journal of the Mechanics and Physics of Solids 58 (2) (2010) 129–144.
[6] B. Loebbecke, R. Knitter, Procurement and quality control of Li_4SiO_4 pebbles for testing of breeder unit mock-ups. Fusion Nr. 311, Final report on TW6-TTBB-006-D02, Forschungszentrum Karlsruhe, Technical report, 2007.
[7] S. Zhao, Multiscale Modeling of Thermomechanical Properties of Ceramic Pebbles, Ph.D. Thesis, Karlsruhe Institute of Technology, 2010 http://digbib.ubka.uni-karlsruhe.de/volltexte/1000021237.
[8] J. Christoffersen, M.M. Mehrabadi, S. Nemat-nasser, Micromechanical description of granular material behavior, Journal of Applied Mechanics 48 (1981) 339.
[9] Y. Gan, M. Kamlah, J. Reimann, Computer simulation of packing structure in pebble beds, Fusion Engineering and Design 85 (2010) 1782–1787.
[10] J. Reimann, E. Arbogast, M. Behnke, S. Mueller, K. Thomauske, Thermomechanical behaviour of ceramic breeder and beryllium pebble beds, Fusion Engineering and Design 49–50 (2000) 643–649.